

Hybrid Neural-Genetic and fuzzy logic approach for real-time tuning of PID Controller to improve the System frequency response of AVR System

M.W. Mustafa¹, Abdullah J. H. Al Gizi^{2*}

¹Faculty of Electrical Engineering, Universiti Teknologi Malaysia, 81310 Johor, Malaysia

² Faculty of Electrical Engineering, Universiti Teknologi Malaysia, 81310 Johor, Malaysia
abdullahgizi@gmail.com

Abstract: Optimal tuning of proportional–integral–derivative (PID) controller parameter is necessary for thematic factory operation of an automatic voltage regulator (AVR) system. This study presents a novel combined genetic algorithm (GA), radial-basis function network (RBF) identification and fuzzy logic control approaches to determine the optimal PID controller parameters in AVR system. The problem of obtaining the optimal AVR and PID controller parameters is formulated as an optimization problem and RBF tuning by GA is applied to solve the optimization problem. The proposed approach has resulted in AVR and PID controller with a good response. Whereas, RBF tuning by GA for various operating conditions are used to develop the rule base of the Sugeno fuzzy system and design fuzzy PID controller (GRBFF-PID) of AVR system to improve the system response. The GRBFF-PID controller is found to possess excellent features of easy implementation, stable convergence characteristic, good computational efficiency and high-quality solution. Our simulation provides high sensitive response (~0.05 sec) of an AVR system compared to the real-code genetic algorithm (RGA), a linear-quadratic regulator (LQR) method and GA. We assert that GRBFF-PID is highly efficient and robust in improving the system frequency response of an AVR system.

[Kharkwal G, Mehrotra P, Rawat YS. **Taxonomic Diversity of Understorey Vegetation in Kumaun Himalayan Forests.** *Life Sci J* 2013;10(4):2946-2957]. (ISSN:1097-8135). <http://www.lifesciencesite.com>. 393

Keywords: AVR, GA, GRBRF-PID, Sugeno fuzzy system, RBF

1. Introduction

The major purpose of the AVR is to control the terminal voltage by regulating the generator exciter voltage. The AVR must keep path of the generator terminal voltage all the time under any load and operational conditions, in order to keep the voltage within pre-established limits. Researches concerning the improvement of the search process to control system engineering problems proposed different approaches to get better solutions. Devaraj and Selvabala [1] suggested a new design method for determining the PID controller parameters of the AVR system using the real coded genetic algorithm method. Kim et al. presented a hybrid GA and bacterial foraging approach to tune the PID controller of an AVR [2]. Valarmathi et al. proposed enhanced GA for PI controllers tuning in pH process [3]. Genetic algorithm (GA) is one of these widely used approaches since it improved its ability for solving optimization problem [2-4]. Genetic algorithms can be found in many applications in biogenetics, engineering, economics, manufacturing, mathematics, physics, chemistry, computer science, and other fields. For instance, GA can be applied to discuss the data classification, fuzzy modeling and Omni-directional robot design problems [5].

[6] During this paper a neuro-fuzzy primarily based methodology is projected to scale back the degree of the uncertainty within the reliability indices

and thus to judge the reliability of the composite power systems exactly. Additionally use of RBF-NN as a result of powerful characteristic to find out any nonlinear mapping between two states. [7] In this study, a stochastic multi objective framework is proposed for distribution feeder reconfiguration (DFR). The proposed multi objective framework will at the same time optimize competitive objective functions as well as total power losses, voltage deviation and total cost. For every settled state of affairs, a multi objective formulation supported the adaptive changed particle swarm improvement (AMPSO) is enforced for every settled state of affairs of it.

[8] Propose, a new hybrid technique supported teacher learning algorithmic rule (TLA) and artificial neural network (ANN) is planned to develop a correct model to analyze short-term load forecasting more precisely. Additionally, in an endeavor to settle on the foremost satisfying options from the set of input variables, a completely unique feature-selection approach supported fuzzy agglomeration and fuzzy set theory is proposed and utilized sufficiently.

Dacheng and Xiaoye proposed the application of PID controller based on GA optimization to control valve in hydraulic system with vertical load [9]. Yu et al. introduced new design method of PID controller based on improved GA for PMSM Servo system. The PMSM is vastly used in modern AC servo system due

to its advantages such as high efficiency, high power density and high performance in wide range speed [10],[11]This paper proposes a new probabilistic framework based on 2m Point Estimate Method (2m PEM) to consider the uncertainties in the optimal energy management of the Micro Grids (MGs) including different renewable power sources .

[12]In this study, the operating benefits of considering thermal recovery and hydrogen production in the economic model of a grid-parallel proton exchange membrane fuel cell power plant (PEM-FCCP) are investigated. The objective functions to be optimized are the total active power losses. [13]This paper suggests a new stochastic method based on point estimate method (PEM) to consider the uncertainty effects in the optimal capacitor placement problem. In this regard, a novel self-adaptive modification approach based on Honey Bee Mating Optimization (HBMO) algorithm is proposed to enhance the total ability of the algorithm effectively.

The PID controller quality will affect significantly the system performance, thus obtaining the PID system parameters is very important. [10] and [14] studied an improved GA (IGA) for the PIO controller based on traditional GA (TGA).The global searching ability and the convergence speed of the IGA are remarkably improved by using real-coded chromosomes scheme [15], and protecting strategies of the best individual [14], accepting immigrations, as well as employing adaptive crossover and mutation operators. On the other hand, arithmetical optimization techniques like gradient descent technique can be applied to get the PID controllers limits. They need some quickly calculations, but with a variable answer surface, these techniques are highly responsive to starting points and often meet to local optimum solutions or deviate in total. In [16], a best PID controller for a universal second-order system has been improved using linear-quadratic regulator (LQR) method. This approach requires a good selection of weighting functions for acceptable performance. On the other hand, neural networks have been widely used in the identification, estimation, and control of nonlinear systems [17]. In addition, nonlinear H ∞

control using radial basis function (RBF) neural networks has been proposed in [18, 19]. Computation techniques such as GA and PSO [20, 21] have been applied to obtain the best controller parameters. Gaing [22] suggested a new design method for determining the PID controller parameters of the AVR system using the particle swarm optimization (PSO) method. PSO is a population-based optimization technique, which is enthused by social performance patterns of organisms such as bird flocking and fish schooling. Whereas, both GA and PSO subject from computational burden and memory condition, they are not appropriate for on-line applications. To overcome the above complexities, we report the design of a novel method by integrating the Sugeno fuzzy system rule base and the AVR system fuzzy PID controller (GRBFF-PID) for enhancing the system response.

2. Problem statement

2.1 Modeling of AVR system

In a synchronous generator, the terminal voltage is kept constant at different levels by using an AVR. The AVR system consists of four major components namely exciter, amplifier, generator, and sensor as shown in Figure 1. An increase in the generator reactive power load is accompanied by a drop in the terminal voltage. A PID controller is used to minimize the error and to achieve improved dynamic response. The PID controller consisting of proportional, integral and derivative manage devices are efficiently used together to place the manipulated variable at the set point.

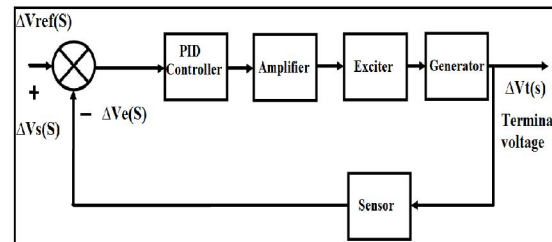


Figure 1. Block diagram of AVR system along with PID controller

Table 1. The transfer function of AVR components

component	Transfer function	Parameter limits
Amplifier	$TF_{amplifier} = K_a / (1 + \tau_a s)$	$10 < K_a < 40$ $0.02 s < \tau_a < 1 s$
exciter	$TF_{exciter} = K_e / (1 + \tau_e s)$	$1 < K_e < 10$ $0.4 s < \tau_e < 1 s$
generator	$TF_{generator} = K_g / (1 + \tau_g s)$	K_s depend on the load (0.7-1.0) $1 s < \tau_g < 2 s$
sensor	$TF_{sensor} = K_s / (1 + \tau_s s)$	$0.001 s < \tau_s < 0.06 s$

The transfer function of the PID controller is given by,

$$G(s) = K_p + \frac{K_i}{s} + K_d s \tag{1}$$

Equations (2) represent the transfer function of AVR systems with PID control. The AVR excellence affects the voltage level through steady-state process and diminishes the voltage oscillations during fleeting periods moving the overall stability of the system.

$$\frac{\Delta V_r(s)}{\Delta V_{ref(s)}} = \frac{(s^2 K_d + s K_p + K_i)(K_v K_g K_s)(1 + s \tau_c)}{s(1 + s \tau_c)(1 + s \tau_e)(1 + s \tau_s) + (K_v K_g K_s K_i)(s^2 K_d + s K_p + K_i)} \tag{2}$$

2.2 Optimization of controller parameters

The acceptable operation of the system is determined by the selection of the best PID controller parameters. Moreover, the selection problem of the PID controller parameters is considered as an optimization problem. The objective function yields,

$$MinF(K_d, K_p, K_i) = (1 - e^{-\beta})(O_{sh} + E_{ss}) + e^{-\beta}(t_s - t_r) \tag{3}$$

The $MinF(K_d, K_p, K_i)$ uses a combination of transient response counting rise time overshoot, settling time and steady-state error. The satisfaction of the designer needs can be achieved by choosing suitable value of the weighting factor β . Therefore, the optimization problem boils down to the following constraints,

$$\begin{aligned} K_p^{min} &\leq K_p \leq K_p^{max} \\ K_i^{min} &\leq K_i \leq K_i^{max} \\ K_d^{min} &\leq K_d \leq K_d^{max} \end{aligned} \tag{4}$$

To search for the optimum values of the controller parameters, GA is applied to the above optimization problem. The proposed GA is given in next section.

2.3 3. Proposed GA

GA is a search algorithm that can optimize PID parameters based on the technicalities of natural selection and genetics. It combines solution evaluation with randomized, structured exchange of information between solutions to obtain optimality [23]. Preliminary with an initial population, the GA uses the information involved in the present population and discovers new individuals by generating offspring using the three genetic operators namely, reproduction, crossover and mutation, which can then replace the old generation members. After several generations, the algorithm converges to the best chromosome, which hopefully represents the optimum or near optimal solution. The details of the genetic operators used in the proposed GA are given in Table 1.

Reproduction

According to their fitness functions, the individuals selected from the population; higher the

fitness, more chances for an individual to be chosen for the next generation. Currently, there are three main types of selection methods: ranking method, fitness balanced selection, and contest or tournament selection. This work used tournament selection [1] where ‘n’ individuals are selected randomly from the population, and the best of the ‘n’ is inserted into the new population for additional genetic processing. This process is frequent until the mating pool is filled. Contests are often held between pairs of individuals, although larger contests can be used.

Crossover operation

The crossover operator is mostly responsible for global search property of the GA. Crossover combines substructures of two-parent chromosomes to produce new structures, with the selected probability typically in the range of 0.6–1.0. One interesting feature of crossover operators is the dependency of the created point depends on the location of both parents. If both parents are close to each other, the new point will also be close to the parents. On the other hand, if parents are far from each other, the search is more like a random search [1].

Mutation operation

New genetic material insert into the population by the mutation operator. Mutation randomly changes a variable with a little likelihood. ‘Uniform mutation’ operator is used in this work. In consistent mutation, the variable is set to a consistent random number between the variable’s lower and upper limits.

3.1 GA implementation for PID controller tuning

while apply GA to obtain the optimal PID controller parameters needs two major subjects to be addressed:

- Symbol of the choice variables and
- Arrangement of the fitness function.

Variable representation

Candidate solutions for everyone in the genetic population are represented. For the PID controller-tuning problem, the elements of the solution consist of integral gain, K_i , proportional gain K_p and derivative gain K_d . Floating-point numbers are used to represent the variables in the proposed GA population. The computer space required to store the population is reduced by the direct representation of the solution variables. Moreover, there is no need to convert the solution variables to the binary string, which leads to increase the GA efficiency. The parameters values (0.6255, 0.2562, 0.1523) that obtained from direct tuning of GA to RBF identification program to optimal tuning of the PID controller parameters is necessary for thematic factory operation of automatic voltage regulator (AVR) system.

Fitness function

The fitness is defined as the non-negative Figure of value to be maximized. It is used to evaluate the performance of everyone in the population. The fitness is associated in a straight line with the object function value. The problem using the parameter set by individual evaluation is accomplished by calculating the performance criteria given by equation (3). The consequence of the presentation criterion computation is used to compute the fitness value of the individual. The fitness function is the mutual of the presentation criterion $F(K_d, K_p, K_i)$ given in equation (3). Hence, the minimization of performance criteria given by (3) is transformed to a fitness function to be maximized as,

$$Fitness = \frac{k}{F(K_d, K_p, K_i) * ITAE} \tag{5}$$

Where k is constant. $ITAE$ is an integral of time multiplied by absolute –error value. This is used to amplify (1/F) the value of which is usually small, so that, the chromosome fitness value will be in a wider range.

2.4 4. RBF Neural Network

In a synchronous In a synchronous generator, an AVR is used to keep the terminal voltage constant at different levels. The AVR system comprised of four main components such as amplifier, exciter, generator and sensors. The outer loop is a self-tuning PID voltage controller based on the radial basis function neural network to provide the ability to adapt for uncertain load and system conditions. Moody et al. proposed a feed-forward two- layered RBF neural network with one single hidden layer to mimic the systematic arrangement of restrictive readjustment in the human mind [18]. Whereas the RBF neural network produces the strongest response near the center of the Gaussian kernel function where each hidden node in the input data space can be regarded as a local detector [24-26] and the RBF neural network is deliberative as local estimation model for the controlled processes. Furthermore, the input samples for RBF neural network do not require a special distribution. In addition, RBF possess an on-line learning and quick converges. Consequently, the control field for implementing the real time manipulation concentrates on the neural network. The RBF is exploited to achieve the best parameters of the controller to maintain the system error zero [27]

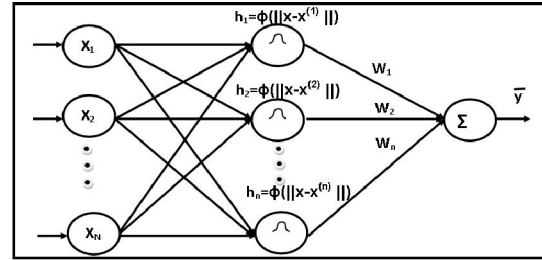


Figure 2. Block diagram of RBF neural network structure

From general block diagram of radial-basis function neural network shown in Figure2, the inputs are n denoted as $X = [x_1, x_2, \dots, x_n]^T$ in vector form. Here is a vector $H = [h_1, h_2, \dots, h_m]^T$ with m elements in the hidden layer. The h_m is named the radial-basis function, where the operator $\|\cdot\|$ represents a p-norm, also known as Euclidean 2-norm. From Gaussian, function form choosing ϕ

$$h_j = \phi(\|X - C_j\|) = e^{-\frac{\|X - C_j\|^2}{2\sigma_j^2}}, \forall j = 1, 2, \dots, m \tag{6}$$

Where the vector $C_j = [c_{j1}, c_{j2}, \dots, c_{jn}]^T$ is the node center of basis function and δ_j its radius accordingly. This is known as Gaussian radial-basis function. The output layer is the manufactured output \bar{y} . Therefore, the network output \bar{y} can be written as follows:

$$\bar{y} = \sum_{j=1}^m w_j \phi(\|X - C_j\|) \tag{7}$$

Where w_j are real number parameters, $\forall j = 1, 2, \dots, m$, are the weights.

The error $(y(k) - \bar{y}(k))$ between system output response $y(k)$ and RBF output $\bar{y}(k)$ is used to regulate the network's parameters. Moreover, this neural network effectiveness is evaluated by a performance function defined as the squared estimation error:

$$J_i = \frac{1}{2} [(y(k) - \bar{y}(k))]^2 \tag{8}$$

The gradient descent method is then applied with the updating algorithms to get output weight, node center and radius parameter stated as follows:

$$w_j(k) = w_j(k-1) + \eta[(y(k) - \bar{y}(k))]h_j + \gamma[w_j(k-1) - w_j(k-2)] \tag{9}$$

$$\Delta \sigma_j = [y(k) - \bar{y}(k)] w_j h_j \frac{\|x - c_j\|^2}{\sigma_j^3} \quad (10)$$

$$\Delta \sigma_j(k) = \sigma_j(k-1) + \eta \Delta \sigma_j + \gamma [\sigma_j(k-1) - \sigma_j(k-2)] \quad (11)$$

$$\Delta c_{ji} = [y(k) - \bar{y}(k)] w_j \frac{x_j - c_{ji}}{\sigma_j^2} \quad (12)$$

$$c_{ji}(k) = c_{ji}(k-1) + \eta \Delta c_{ji} + \gamma [c_{ji}(k-1) - c_{ji}(k-2)] \quad (13)$$

γ is the momentum factor, and η is the learning rate for the neural network. This updating algorithm includes the learning capability. The PID controller parameters K_p, K_i, K_d are regulated by the RBF neural network. A short analysis of RBF-PID controller is given as follows; the system error $e(k)$ for the unit negative feedback control system can be written as

$$e(k) = r(k) - y(k) \quad (14)$$

where $r(k)$ is the reference command. Furthermore, the efficiency of this adaptive controller is estimated by a performance function defined as the squared error:

$$E(k) = \frac{1}{2} e^2(k) \quad (15)$$

The adaptive controller output $u(k)$ can be represented in the updating algorithm as:

$$u(k) = u(k-1) - \Delta u(k) \\ = u(k-1) + k_p \cdot e_p(k) + k_i \cdot e_i(k) + k_d \cdot e_d(k) \quad (16)$$

Where K_p, K_d and K_i are proportional gain, derivative gain, and integral gain respectively. The $e_p(k), e_i(k)$ and $e_d(k)$ are defined as proportional error function, integral error function, and derivative error function respectively as follows: $e_p(k) = e(k)$ (17)

$$e_d(k) = e(k) - 2e(k-1) + e(k-2) \quad (18)$$

$$e_i(k) = e(k) - 2e(k-1) + e(k-2) \quad (19)$$

The gradient descent method is applied with the chain rule to infer the regulating rules for the K_p, K_d and K_i to minimize the performance index function $E(k)$ as follows:

$$\Delta k_p = -\mu \frac{\partial E}{\partial k_p} = -\mu \frac{\partial E}{\partial y} \frac{\partial y}{\partial u} \frac{\partial u}{\partial k_p} = \mu e(k) \cdot \frac{\partial y}{\partial u} \cdot e_p(k) \quad (20)$$

$$\Delta k_i = -\mu \frac{\partial E}{\partial k_i} = -\mu \frac{\partial E}{\partial y} \frac{\partial y}{\partial u} \frac{\partial u}{\partial k_i} = \mu e(k) \cdot \frac{\partial y}{\partial u} \cdot e_i(k) \quad (21)$$

$$\Delta k_d = -\mu \frac{\partial E}{\partial k_d} = -\mu \frac{\partial E}{\partial y} \frac{\partial y}{\partial u} \frac{\partial u}{\partial k_d} = \mu e(k) \cdot \frac{\partial y}{\partial u} \cdot e_d(k) \quad (22)$$

Where, $\frac{\partial y}{\partial u}$ is Jacobean matrix denoting the sensitivity relating system output $y(k)$ to controller output $u(k)$ and, μ is the learning rate for the adaptive PID algorithm. The inputs, output response are three inputs in the RBF algorithm, output response $x_1 = y(k)$ delayed output response $x_2 = y(k-1)$, and controller output $x_3 = u(k)$. The manufactured output $\bar{y}(k)$ of RBF will approach the system output $y(k)$ after on-

line learning. Therefore $\frac{\partial \bar{y}(k)}{\partial u(k)}$, is very close to $\frac{\partial y(k)}{\partial u(k)}$ and one can conclude from (9) and (10),

$$\frac{\partial y(k)}{\partial u(k)} \approx \frac{\partial \bar{y}}{\partial x_3} = \frac{\partial}{\partial x_3} \sum_{j=1}^m w_j e^{-\frac{\|x - c_j\|^2}{2\sigma_j^2}} \\ = \sum_{j=1}^m w_j h_j \frac{\partial}{\partial x_3} \left(-\frac{\|x - c_j\|^2}{2\sigma_j^2} \right) \\ = \sum_{j=1}^m w_j h_j \frac{\partial}{\partial x_3} \left(-\frac{X^T X - X^T C_j - C_j^T X + C_j^T C_j}{2\sigma_j^2} \right) \quad (23) \\ = \sum_{j=1}^m w_j h_j \left(-\frac{2x_3 - 2c_{j3}}{2\sigma_j^2} \right) \\ = \sum_{j=1}^m w_j h_j \frac{c_{j3} - u(k)}{\sigma_j^2}$$

Thus, the updating algorithm for the adaptive PID based on RBF can be derived as:

$$\Delta k_p = \mu \cdot e(k) \cdot e_p(k) \cdot \sum_{j=1}^m w_j h_j \frac{c_{j3} - u(k)}{\sigma_j^2} \quad (24)$$

$$\Delta k_i = \mu \cdot e(k) \cdot e_i(k) \cdot \sum_{j=1}^m w_j h_j \frac{c_{j3} - u(k)}{\sigma_j^2} \quad (25)$$

$$\Delta k_d = \mu \cdot e(k) \cdot e_d(k) \cdot \sum_{j=1}^m w_j h_j \frac{c_{j3} - u(k)}{\sigma_j^2} \quad (26)$$

The PID parameters K_p, K_d and K_i are automatically readjusted by on-line learning algorithm of RBF and (24)-(26) to keep the system error, $e(k)$ zero

2.5 Simulation results

5.1 Performance of GA-PID controller

Next, the proposed GA was applied to optimize PID controller parameters. The software for the proposed GA was written in MATLAB and executed on a laptop Intel core(TM) 2 Duo CPU 5550@1.83GHz and 3GB. Integral gain K_i Proportional gain K_p and derivative gain K_d are the

optimization variables. The primary population is produced randomly among the variable's lower and upper restrictions. To evaluate the fitness value of each controller parameters set the fitness function given by (5) is used to evaluate the fitness value of each set of controller parameters. Simulation was conducted with different values of β . The GA performance for various values of crossover and mutation likelihood in the ranges 0.6–1.0 and 0.001–0.1 respectively, was evaluated. The top consequences are obtained with the following control parameters. Generations' number: 75, Population size: 30, Crossover probability: 0.6, Mutation probability: 0.001. The GA took 33.72s to reach the optimal solution. The GA convergence characteristics are shown in Figure3. During this stage, the main focus of GA is to find feasible solutions of the problem. It can be noted that the value increases slowly and stabilizes near the optimum value that most individuals in the population trying to reach. The controller parameters optimal values obtained by using the proposed GA for different values of β are given in Table 2.

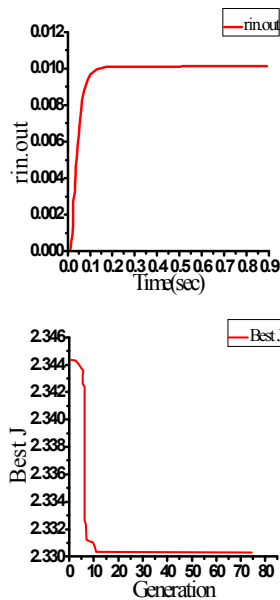


Figure 3. Shows the convergence characteristics of GA algorithm

Table 2. Optimal value the control parameter obtained using the proposed GA

Kpdi			Bestfi	Best_J	β
K_d	K_p	K_i			
0.2768	0.6877	0.1629	0.428	2.3366	0.5
0.2968	0.5563	0.1629	0.4293	2.3291	1
0.2801	0.6329	0.1785	0.4280	2.3366	1.5

5.2 Performance of RBF-PID controller AVR tuning

The proposed methodology for PID controller tuning was tested on an AVR system. The AVR system consists of generator, exciter, amplifier and sensor. The parameters of AVR system are selected as following: $K_a=10$, $K_e=K_g=K_s=1.0$, $\tau_a=0.1$, $\tau_e=0.4$, $\tau_s=0.01$ and $\tau_g=1.0$ only K_g and τ_g are load dependent. MATLAB Simulink was used to simulate the AVR system. The MATLAB-Simulink model of AVR system with PID controller is shown in Figure4. The first time PID controller was tuned using GRBF-NN (RBF-NN tuning by GA), second time PID controller was tuned using (RBF-NN tuning by RAG). A step reference voltage of 0.01 p.u is applied, and the step response of change in terminal voltage of AVR system in the presence of PID controller is shown in Figure5. From the Figure, it is observed that the AVR system response with RBF PID (RBF-NN tuning by GA or RGA) controller increases in a steady state until reaches to reference voltage of 0.01 p.u with little oscillatory mode and large settling time. During this stage, the main concentrates is to find feasible solutions for the problem. Then the value increases slowly and stabilizes near the optimum value with small swing dependent on tuning data to reach that point (GA or RGA with RBF-NN).

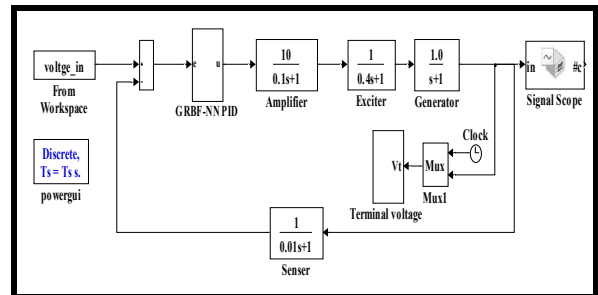


Figure 4. MATLAB-Simulink model of AVR system along with PID controller

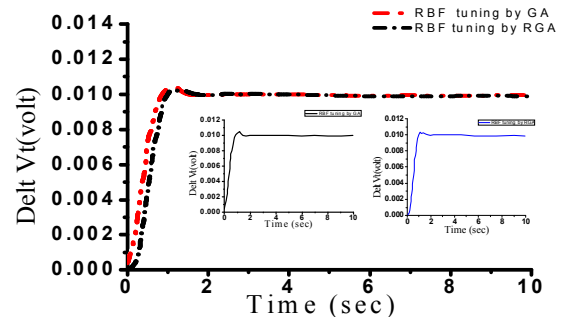


Figure 5. Shows characteristics of RBF PID controller tuning by GA and, RGA [1]

Our simulation results are summarized in Table 3, and the terminal voltage responses are also shown

in Figure6. We find that the proposed RBF-NN tuning by RGA approach minimizes the rise time, reduces settling time and overshoots when compared with the results obtained using methods of LQR, RAG and binary-coded GA [1]. Conversely, GRBF-NN (RBF-NN tuning by GA) results better minimum settling time, less rise time and overshoot in comparison to that obtained using methods of LQR and binary-coded GA [1]. Furthermore, the convergence time achieved by the proposed algorithm is shorter compare to RGA. Figure7 illustrated, the test system includes two completely regular areas connected jointly by two 230 kV lines each of 220 km length. It is specially intended in to study low frequency electromechanical oscillations in big unified power systems [28, 29]. In spite of its little size, it mimics very well the typical systems performance in real process. Every area is equipped with two same performance generators rated 20 kV/900 MVA. The synchronous machines have identical parameters [28, 29] such as $H = 6.5$ s in area 1 and $H = 6.175$ s in area 2 [19].

Thermal plants have the same speed regulators and AVR that contain RBF PID controller tuned using the RGA [1]and GA. To analyses performance of the AVR system under severe disturbances, a three phase fault is applied at the generator terminal and the response of the system was observed. Figure 8 show the system response for the above contingency with RBF PID controller tuned using the RGA [1]and GA. It can be observed that the controller (GRBF-NN) is able to suppress the oscillations in the terminal voltage and provide good damping characteristics. The red line represents area 1 response, while the black line represents area 2 responses. Meanwhile, we wanted from the above results that reached why the fuzzy PID controller is designed using the optimal PID gains obtained by a combined GA and RBF-NN for various operating conditions. This is further employed to develop the rule based of the Sugeno fuzzy system. This algorithm searches for a high-quality solution

effectively and improves the transient response of the AVR system as shown in the section below.

5.3 Development of Sugeno fuzzy model for on line tuning to design PID controller

The optimum PID parameters for real-time operation are obtained by developing Sugeno fuzzy logic model, where, K_e and τ_e are the inputs and K_p , K_d and K_i are the outputs. Eight fuzzy sets for instance ‘very low (VL)’, ‘low(L)’, ‘medium low (ML)’, ‘medium(M)’, ‘medium high (MH)’, ‘high low (HL)’, ‘high medium (HM)’ and ‘high (H)’ are defined for the variable K_e .

Likewise, the fuzzy sets defined for the variable τ_e are ‘very low (VL)’, ‘low (L)’, ‘medium low (ML)’, ‘medium high (MH)’, ‘high (H)’ and ‘very high (VH)’. They are linked with overlapping triangular membership functions. To formulate the table for fuzzy rule, the values of K_e are varied from 2.0 to 9.0 in steps of 1.0 and τ_e are varied from 0.5 to 1 in steps of 0.1. For each combination of K_e and τ_e , the proposed RBF-NN tuning via GA is applied to obtain the optimal values of K_p , K_d and K_i . The fuzzy rule table formulated for K_p , K_d and K_i using the above approach is summarized in Table 4 as (a), (b) and (c), respectively.

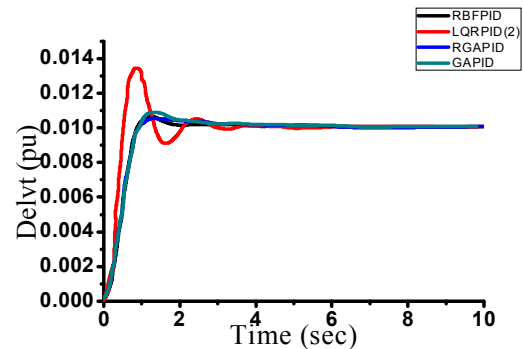


Figure 6. Comparison Step response of GRBF-PID with LQR, RAG and binary-coded GA [1] response

Table 3. Comparison of PID gains and transient response parameters for the different methods.

Method	PID parameters			$T_s (s)$	$T_r (s)$	O_{sh}	$E_{ss}(10^{-5})$
	K_p	K_i	K_d				
LQR[1]	1.01	0.5	0.1	2.3354	0.5004	0.3605	15.007
Binary-coded GA[1]	0.5692	0.2484	0.1258	1.7019	0.8093	0.0586	8.2941
RGA[1]	0.682	0.266	0.179	1.2682	1.0668	0.0004	4.3386
RBF tuning by GA(GRBF-NN)	0.657	0.2958	0.1952	1.3766	1.0024	0.00168	5.3275
RBF tuning binary-coded GA[1]	0.6003	0.2899	0.1626	1.4050	0.9405	0.00195	6.2490
RBF tuning by RGA[1]	0.7136	0.3004	0.2317	1.3849	0.9522	0.00167	5.8305

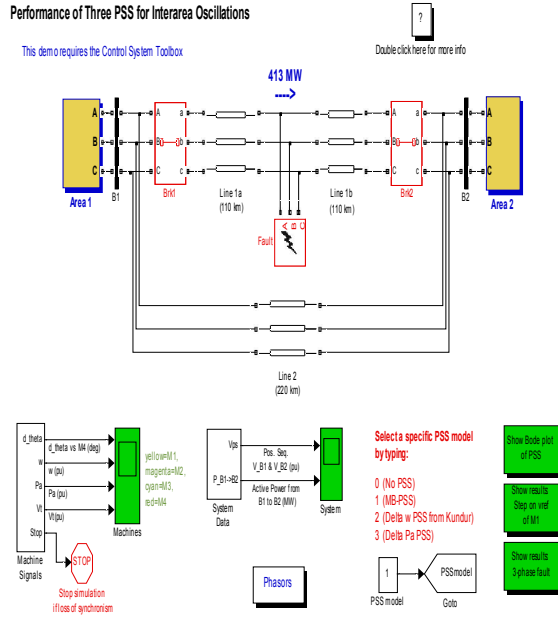


Figure 7. MATLAB-Simulink models test system includes two completely regular areas connected jointly by two 230 kV lines each of 220 km length.

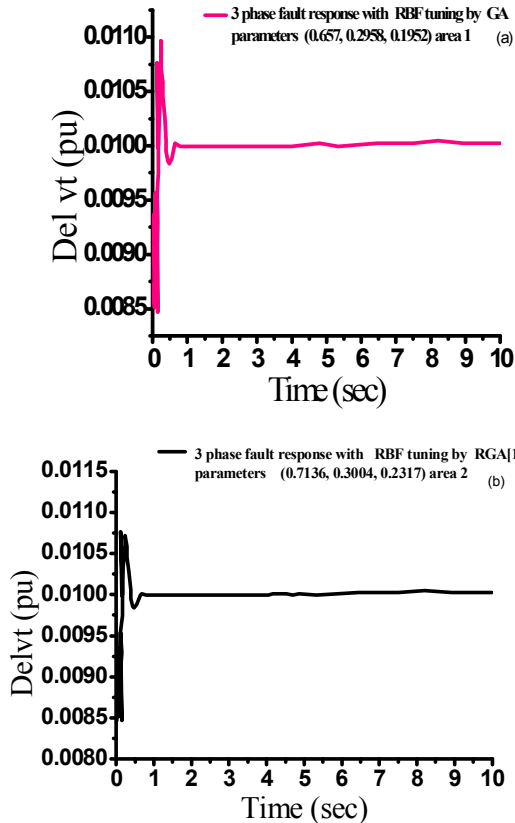


Figure 8.(a), (b) 3 Phase fault response with RBF tuning by GA and RGA [1] parameters

During real-time operation, corresponding to the present operating conditions, the values of K_e and τ_e are found out. For this values of K_e and τ_e , the optimal value of K_p , K_d and K_i can be computed using the fuzzy rule table and the FIS editor Sugeno inference system explained in section 3.1. Depending on the initialization (FIS editor), the inputs of the fuzzy logic controller are K_e , τ_e and the outputs are K_p , K_d and K_i .

The system with three fuzzy logic controllers K_p , K_d and K_i with rule viewer are set in which each controller has two inputs K_e , τ_e and each input has fuzzy set associated with it. The output has 144 fuzzy set rules for K_p , K_d and K_i , and 48 rules for each one parameter as depicted in Figure 9 (a),(b) shown rule viewer and surface viewer of novel GRBFF-PID controller.

MATLAB programming is used for the proposed RBF-NN tuning via GA executed on a Intel core (TM) 2 Duo CPU 5550@1.83GHz and 3GB RAM laptop. The optimal solution of combination is achieved in the duration of 23.79 sec.

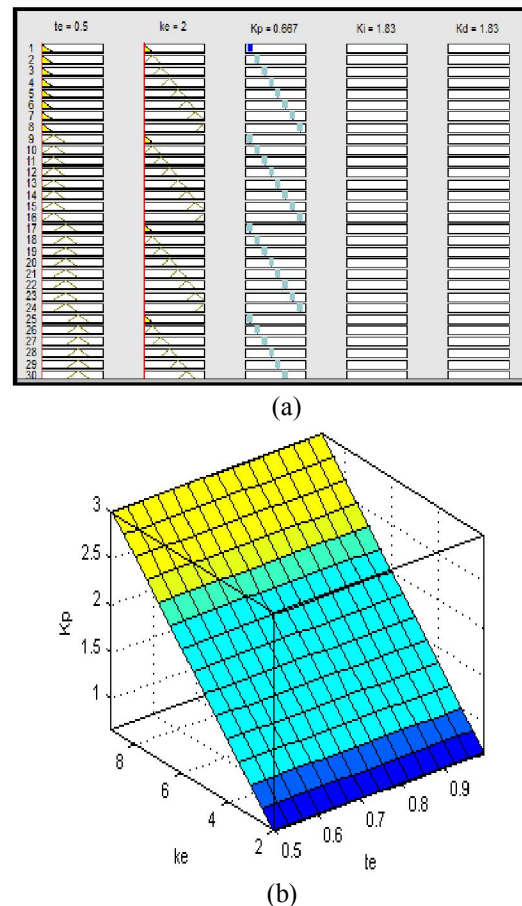


Figure 9.(a), (b) Are Rule and Surface viewer of Sugeno fuzzy PID controller (GRBFF-PID)

Table 4. The fuzzy rule Table formulated for K_p , K_i and K_d using the above approach

τ_e	Very low	Low	Medium Low	Medium high	High	Very high
K_e	0.5	0.6	0.7	0.8	0.9	1
(a) For proportional gain K_p						
Very Low(2)	0.2944	0.6124	0.5980	0.4622	0.4728	0.6079
Low (3)	0.4153	0.3768	0.4796	0.5115	0.4887	0.3817
Medium low (4)	0.2859	0.3304	0.3377	0.3617	0.3662	0.3835
Medium (5)	0.1039	0.2158	0.1085	0.3141	0.3099	0.3477
Medium High (6)	0.1878	0.2422	0.2486	0.2615	0.2715	0.2037
High low(7)	0.1164	0.1123	0.2108	0.1747	0.0988	0.2570
High medium (8)	0.1780	0.1071	0.1967	0.2068	0.2127	0.1705
High (9)	0.1391	0.1355	0.1257	0.0880	0.1823	0.1625
(b) For integral gain K_i						
Very Low(2)	0.4201	0.4280	0.4276	0.4718	0.5110	0.5277
Low (3)	0.2960	0.3060	0.3218	0.3372	0.3594	0.3739
Medium low (4)	0.2424	0.2427	0.2638	0.2671	0.2798	0.2946
Medium (5)	0.2193	0.2112	0.2370	0.2362	0.2397	0.2415
Medium High (6)	0.1902	0.1947	0.2005	0.2114	0.2190	0.2271
High low(7)	0.1749	0.1860	0.1840	0.1937	0.2035	0.1972
High medium (8)	0.1591	0.1650	0.1714	0.1713	0.1787	0.1916
High (9)	0.1497	0.1559	0.1599	0.1731	0.1723	0.1795
(c) For derivative gain K_d						
Very Low(2)	0.0241	0.0378	0.0540	0.2007	0.1916	0.2102
Low (3)	0.1733	0.1436	0.1489	0.0285	0.0284	0.2074
Medium low (4)	0.0697	0.0199	0.0207	0.1572	0.0391	0.0897
Medium (5)	0.0144	0.1069	0.0391	0.0400	0.0221	0.0904
Medium High (6)	0.0877	0.0160	0.0388	0.0170	0.0175	0.1035
High low(7)	0.0710	0.0179	0.0658	0.0776	0.0191	0.0168
High medium (8)	0.0131	0.0669	0.0661	0.0321	0.0146	0.0632
High (9)	0.0353	0.0661	0.0493	0.0192	0.0136	0.0398

5.4 Implementation of Electrical Power Generation

The MATLAB-Simulink model of Electrical Power Generation System along with along with Sugeno fuzzy PID controller (GRBFF-PID) is shown in Figure 10 and the GRBFF-PID controller used with the excitation system is shown in Figure 11. A step reference voltage of 1.38 kV is applied. The GRBFF-PID controller has the ability to hold back the oscillations in the terminal voltage and provide high-quality damping characteristics. The test system includes a generator excitation system, as shown in the appendix, connected by 500 kV lines of 650 km length and a 300 MVA-500/230 kV transformer feeds a 230 kV-250 MW load. THE transmission line is split into two lines. The first line is 350 km length connects between buses B1, B4, and the second one is 300 km length connects between buses B4 and B5. The two circuit breakers of line 1 are CB1 and CB2 and discrete 3-Phase PLL block measures the frequency,

whereas the PLL drives two measurement blocks considering the variable frequency. The first block computes the essential value of the positive-sequence load voltage while the second block computes the active load and reactive powers.

The terminal voltage response of excitation system with GRBFF-PID controller is found to be highly sensitive to a tiny change (time response 0.05 and 2 sec) as shown in Figure 12 (a) and (b). This demonstrates the suitability of the proposed approach to obtain the optimal PID gains during system real-time operation. Our proposed method renders better performance in the rise time, peak overshoot and the steady state error. The responses observed from the present controller have a slight overshoot, which can be improved considerably by increasing the rules number. We establish that the GRBFF-PID controller has better performance in comparison to other controllers.

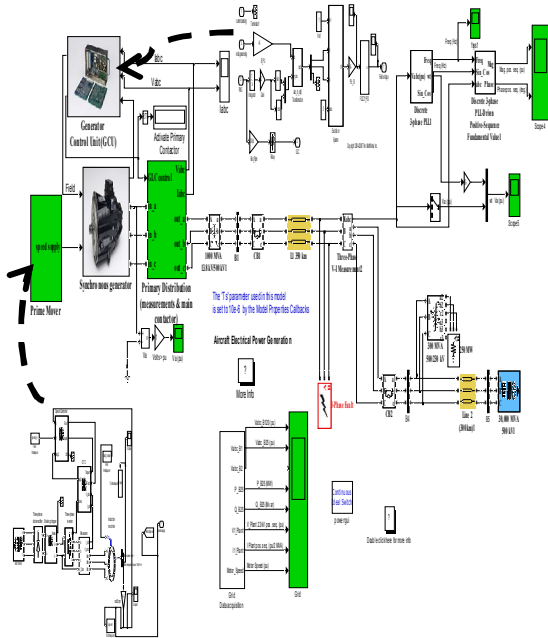


Figure 10. The MATLAB-Simulink model of Electrical Power Generation System along with Sugeno fuzzy PID controller (GRBFF-PID)

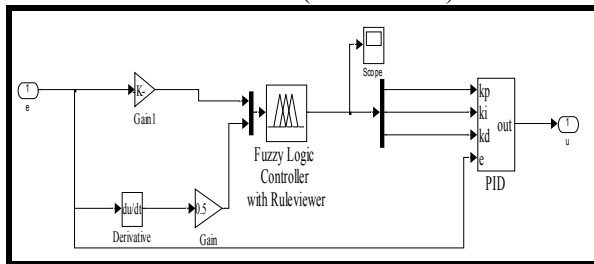


Figure 11 .Sugeno fuzzy PID controllers (GRBFF-PID)

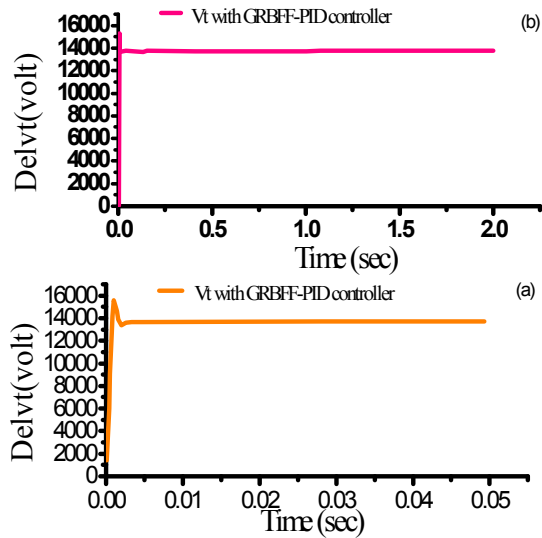


Figure 12 (a)&(b) Terminal voltage response of excitation system with GRBFF-PID controller

Whereas, explanation system frequency responds under the test periodic, as shown in Figure 13.a. are at $t = 1.0$ s, a three-phase to ground fault occurs on the 500 kV bus. The fault is cleared ($t = 1.1$ s). Observe on Scope block how the PLL tracks the changing system frequency (trace) the frequency of the system at the moment of fault, steps down to 59.96Hz, at $t = 1.0$ s, when fault is cleared the frequency 59.968 Hz at $t = 1.1$ s, but the frequency swings between 59.66 and 60.03 Hz until it reaches a steady state frequency 60Hz at 1.42/sec. Figure 13.b. at $t = 1.0$ s, a two-phase to ground fault occurs on the 500 kV busbar. The frequency of the system at the moment of fault, steps down to 59.94Hz, at $t = 1.0$ s, when fault is cleared, steps up to 60.03Hz at $t = 1.1$ s, but the frequency swings between 59.77 and 60.035 Hz until it reaches a steady state frequency 60 Hz at 1.36/sec. Figure 13.c. at $t = 1.0$ s, a single-line to ground fault occurs on the 500 kV bus. The frequency of the system at the moment of fault steps down to 59.88Hz, and up to 60.12Hz at $t = 1.0$ s, when fault is cleared the frequency is 59.965Hz at $t = 1.1$ s but the frequency swings between 59.72 and 60.028 Hz until it reaches a steady state frequency 60Hz at 1.345/sec. Figure 13.d. at $t = 1.0$ s, a two-phase (line to line) fault occurs on the 500 kV bus. The frequency of the system at the moment of fault, the frequency swings between, steps down to 59.94Hz, and steps up to 60.17 Hz at $t = 1.0$ s, when fault is cleared the frequency reaches to 59.96Hz at $t = 1.1$ s but the frequency swings between 59.77 and 60.0148 Hz until it reaches a steady state frequency 60 Hz at 1.325/sec. Whereas, a three-phase to ground fault has higher frequency swing and time steady state than all three types of fault that occur on same bus.

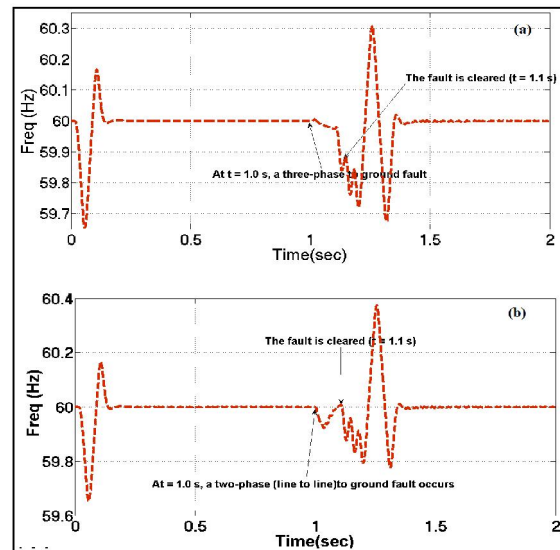


Figure 13 (a) & (b)

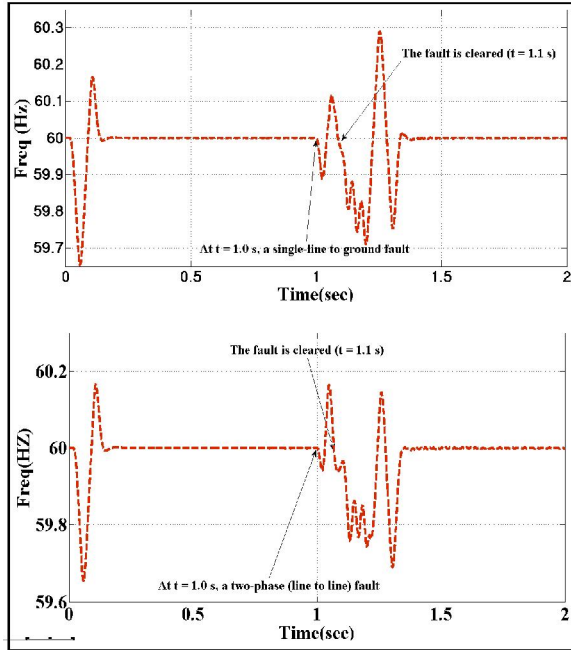


Figure 13 (c) & (d)

2.6 6. Conclusion

We present a combined approach of GA, Sugeno fuzzy logic and RBF-NN to determine the optimal PID controller parameters in AVR system. The RBF-NN is used to enhance the PID parameters obtained from GA to design Sugeno fuzzy PID controller tuned by excitation parameter (K_e, τ_e). The GRBFF-PID controller possess preferable features such as easy implementation, stable convergence characteristic, good computational efficiency and high-quality solution that keeps the system error closer to zero. A novel combination can directly deals with the real variables have been applied to get the optimal parameter of PID fuzzy controller in AVR. Furthermore, the results for the numerical simulation offer a high sensitive response (~0.05 sec) of the AVR system compare to the RGA, LQR and GA, and the RBF and improved the system frequency response. Interestingly, the novel GRBFF-PID controller tracks the set point with small oscillation due to the prime mover speed. The excellent features of our method suggest that the new technique automatically averts the over fitting problem, which is adverse for many optimizations and learning algorithms.

Appendix

Generation parameters					
$P_n (VA)$	1000E6	$f_n [Hz]$	50	Inertia	0.02
$V_n (V_{rms})$	13800	Pairs of poles	2	Internal impedance R(ohm)	0.0204
Damping factor	0	Initial condition [dw,th(deg), ia,ib,ic(A), pha,phb,phc(deg)]	[-99,0 0,0,0 0,0,0]	Sample time	-1
L(H)	0.08104e-3			Regulator gain and time constant	[300, 0.001]
Excitation System					
[vt0 (pu) vf0(pu)]	[1 0]	Low_pass filter time constant	20e-3	[Kf] Tf(s)]	[0.001, 0.]
Exciter [Ke() Te(s)]	[1,0]	Transient gain [Tb(s) Tc(s)]	[0,0]	[Efmin,Efmax(pu),Kp()]	[-2, 2, 0]
Rotor parameters					
$P_n (VA)$	1100	$R_s [\Omega]$	0.435	$f_n [Hz]$	50
$V_n (V_{rms})$	200	$R r' [\Omega]$	0.816	$J [Kg.m^2]$	0.089
η	0.78	$L l r' [H]$	2e-3	$F [N.m.s]$	0.005
cos	0.8	$L l s [H]$	2e-3	p	2
$N(r.p.m)$	3600	$L m [H]$	69.31e-3		

Corresponding Author:

Abdullah Jubair Halboos Al Gizi

Received his B. Eng Degree (1995), M. Sc. (2003) from University of Technology Baghdad. He is currently a PhD student at Faculty of Electrical Engineering, UTM, Johor Bahru, E-mail: abdullahalhazi@gmail.com abdullah969@yahoo.com

References

1. Devaraj, D. and B. Selvabala, *Real-coded genetic algorithm and fuzzy logic approach for real-time tuning of proportional-integral - derivative controller in automatic voltage regulator system*. Generation, Transmission & Distribution, IET, 2009. **3**(7): p. 641-649.
2. D.H. Kim, A.A., and J.H. Cho, *A hybrid genetic algorithm and bacterial foraging approach for global*

- optimization*. Int. J. Inf. Sci., 2007. **177**(18): p. 3918–3937.
3. K. Valarmathi, D.D., and T.K. Radhakrishnan, *Enhanced genetic algorithm based proportional integral controller tuning for pH process*. Instrument. Sci. Technol., 2007. **35**(6): p. 619-635.
 4. Nasir, A.N.K., et al. *A novel hybrid spiral-dynamics bacterial-foraging algorithm for global optimization with application to control design*. in *Computational Intelligence (UKCI), 2012 12th UK Workshop on*. 2012.
 5. M.Shady. Gadoue, D.G.a.J.W.F., *Genetic Algorithm Optimized PI and Fuzzy Mode Speed Control for DTC drives*. London, U.K Proceedings of the World Congress on Engineering 2007, 1, WCE 2007 p. 2007, 1, WCE 2007, July 2-4, 2007. , 2007.
 6. Kavousifard, A. and H. Samet, *Consideration effect of uncertainty in power system reliability indices using radial basis function network and fuzzy logic theory*. Neurocomput., 2011. **74**(17): p. 3420-3427.
 7. T. Niknam, A.K.F., Jamshid Aghayi, *Scenario-Based Multiobjective Distribution Feeder Reconfiguration considering Wind Power Using Adaptive Modified PSO*. IET Renewable 2012. **6**(4): p. 236-247.
 8. Kavousi-Fard, A., *A new fuzzy-based feature selection and hybrid TLA-ANN modelling for short-term load forecasting*. Journal of Experimental & Theoretical Artificial Intelligence, 2013: p. 1-15.
 9. Xiaoye, G.D.a.Q., *The Application of PID Controller Optimized by Genetic Algorithm in Valve-Controlling Asymmetrical Cylinder System*. International Conference on Electronic & Mechanical Engineering and Information Technology, 2011.
 10. R. Yu, Z.C.a.H.Z., *Optimal PID Controller Design in PMSM Based on Improved Genetic Algorithm* 2nd International Conference on Industrial Mechatronics and Automation 2010.
 11. Baziar, A. and A. Kavousi-Fard, *Considering uncertainty in the optimal energy management of renewable micro-grids including storage devices*. Renewable Energy, 2013. **59**(0): p. 158-166.
 12. Niknam, T. and A. Kavousifard, *Impact of thermal recovery and hydrogen production of fuel cell power plants on distribution feeder reconfiguration*. Generation, Transmission & Distribution, IET, 2012. **6**(9): p. 831-843.
 13. A Kavousi-Fard, T.N., *Considering uncertainty in the multi-objective stochastic capacitor allocation problem using a novel self adaptive modification approach*. Electric Power Systems Research (EPSR), 2013. **103**: p. 16-27.
 14. L. Fan, E.M.J., *Design for auto-tuning PID controller based on genetic algorithms*. Industrial Electronics and Applications., 2009: p. 1924-1928.
 15. H. Hu, Q.H., Z. Lu, D.Xu, *Optimal PID Controller Design in PMSM Servo System Via Particle Swarm Optimization*. Industrial Electronics Society, , Nov. 2005: p. 79-83,.
 16. Gwo-Ruey, Y. and H. Rey-Chue. *Optimal PID speed control of brush less DC motors using LQR approach*. in *Systems, Man and Cybernetics, 2004 IEEE International Conference on*. 2004.
 17. F. Pourboghrat, H.P., Ziqian Liu, and F.Farid., *Dynamic neural Networks for modeling and control of nonlinear systems*. Intelligent Automation and soft computing, 2003. **19**(2): p. 61-70.
 18. Darken, J.M.a.C., *Learning with Localized Receptive Fields*. Proceedings of the 1988 Connectionist Models Summer School, 1988: p. 133-143.
 19. M.S.Ahmed, *Neural controllers for nonlinear state feedback L2- gain control*. IEE Proceedings of Control Theory Applications, 2000. **147**(3).
 20. Khandani, K., A.A. Jalali, and M. Alipoor. *Particle Swarm Optimization based design of disturbance rejection PID controllers for time delay systems*. in *Intelligent Computing and Intelligent Systems, 2009. ICIS 2009. IEEE International Conference on*. 2009.
 21. Krohling, R.A. and J.P. Rey, *Design of optimal disturbance rejection PID controllers using genetic algorithms*. Evolutionary Computation, IEEE Transactions on, 2001. **5**(1): p. 78-82.
 22. Zwe-Lee, G., *A particle swarm optimization approach for optimum design of PID controller in AVR system*. Energy Conversion, IEEE Transactions on, 2004. **19**(2): p. 384-391.
 23. Goldberg, D., *Genetic algorithms in search, optimization and machine learning*. Addison-Wesley, 1989.
 24. S.N. Qasem, S.M.S., *Memetic Elitist Pareto Differential Evolution algorithm based Radial Basis Function Networks for classification problems*. Applied Soft Computing, 2011. **11**(1): p. 5565–5581.
 25. S.N. Qasem, S.M.S., *Radial basis function network based on time variant multi-objective particle swarm optimization for medical disease diagnosis*. Applied Soft Computing, 2011. **11**(1): p. 1427–1438.
 26. N. A. Al-geelani, M.A.M.P., R. Q. Shaddad *Characterization of acoustic signals due to surface discharges on H.V. glass insulators using wavelet radial basis function neural networks* Applied Soft Computing, 2012. **7**(2): p. 1327-1338.
 27. Yao-Lun, L., et al. *Design an Intelligent Neural-Fuzzy Controller for Hybrid Motorcycle*. in *Fuzzy Information Processing Society, 2007. NAFIPS '07. Annual Meeting of the North American*. 2007.
 28. Klein, M., et al., *Analytical investigation of factors influencing power system stabilizers performance*. Energy Conversion, IEEE Transactions on, 1992. **7**(3): p. 382-390.
 29. Kundur, P., *Power System Stability and Control*. Vol. Example 12.6. 1994: McGraw-Hill.